Electrochimica Acta 56 (2011) 4685–4690

Contents lists available at ScienceDirect

Electrochimica Acta

journal homepage: www.elsevier.com/locate/electacta

TiO_2-graphene nanocomposite for electrochemical sensing of adenine and guanine

Yang Fan[a,*], Ke-Jing Huang[a], De-Jun Niu[a], Chun-Peng Yang[b], Qiang-Shan Jing[a]

[a] College of Chemistry and Chemical Engineering, Xinyang Normal University, Xinyang 464000, PR China
[b] Qingdao Institute of Bioenergy and Bioprocess Technology, Chinese Academy of Sciences, Qindao 266101, PR China

ARTICLE INFO

Article history:
Received 13 December 2010
Received in revised form 24 February 2011
Accepted 25 February 2011
Available online 4 March 2011

Keywords:
Graphene
TiO_2-graphene nanocomposite
Adenine
Guanine
Electrochemical sensor

ABSTRACT

TiO_2-graphene nanocomposite was prepared by hydrolysis of titanium isopropoxide in colloidal suspension of graphene oxide and in situ hydrothermal treatment. It provides an efficient and facile approach to yield nanocomposite with TiO_2 nanoparticles uniformly embedded on graphene substrate. The electrochemical behavior of adenine and guanine at the TiO_2-graphene nanocomposite modified glassy carbon electrode was investigated. The results show that the incorporation of TiO_2 nanoparticles with graphene significantly improved the electrocatalytic activity and voltammetric response towards these species comparing with that at the graphene film. The TiO_2-graphene based electrochemical sensor exhibits wide linear range of 0.5–200 μM with detection limit of 0.10 and 0.15 μM for adenine and guanine detection, respectively. The excellent performance of this electrochemical sensor can be attributed to the high adsorptivity and conductivity of TiO_2-graphene nanocomposite, which provides an efficient microenvironment for electrochemical reaction of these purine bases.

1. Introduction

Graphene-based electrochemical sensors and biosensors have recently received increasing attention in the field of electroanalysis [1–4], such as direct electrochemistry of enzymes [5–9] and small biomolecules detection [10–13]. Owing to its extraordinary electronic transport properties and high electrocatalytic activities, graphene greatly promotes the electrochemical reactivity of biomolecules on the modified electrode surface [1,2]. Furthermore, the unique two-dimensional crystal structure of graphene makes it extremely attractive as a support material for metal and metal-oxide catalyst nanoparticles [14]. These graphene-based hybrid materials have shown greater versatility as enhanced electrode materials for electrochemical sensors and biosensors applications [15,16].

Due to its good biocompatibility, high conductivity and low cost, TiO_2 in various forms such as nanoparticles, nanoneedles and nanotubes, has become an attractive electrode material for electrochemical sensors and biosensors applications [17–24]. Recently, Liu et al. fabricated the electrochemical sensor by casting TiO_2 nanotubes film onto glassy carbon electrode (GCE) surface. The TiO_2 nanotubes film showed to be capable of improving the mass transport and electron transfer between dopamine and the electrode surface [23]. Bao et al. demonstrated that glucose oxidase (GOD) can be immobilized on porous TiO_2 to fabricate glucose biosensor. This biosensor exhibited good direct electrochemistry without any electron mediator, as well as good sensitivity and fast response time towards glucose detection [24]. On the other hand, the photophysical and electrochemical properties of TiO_2 have shown to be greatly improved in TiO_2-graphene hybrid materials [14,25–28]. Li and coworkers observed significant enhancement in the reaction rate using TiO_2-graphene as photocatalyst for photodegradation of methylene blue [25]. Liu and coworkers reported that TiO_2-graphene nanocomposite can remarkably improve the Li-ion insertion/extraction property and specific capacity of Li-ion battery [26]. In these studies, such excellent performance can be reasonably attributed to the good adsorptivity and conductivity of the TiO_2-graphene nanocomposite. Most recently, we reported the TiO_2-graphene nanocomposite prepared by hydrothermal method using graphene as templates to immobilize TiO_2 nanoparticles [29]. The as-prepared TiO_2-graphene nanocomposite exhibited remarkable electrochemical sensing performance towards dopamine detection with wide linear range, high selectivity and low detection limit, which opened a new platform for electrochemical sensors and biosensors design.

Adenine (A) and guanine (G) are components of DNA, and most of the current electroanalytical protocols for DNA detection are based on these two electroactive species [30]. However, adenine and guanine exhibit slow direct electron transfer and irreversible absorption on the electrode surface, which lead to low sensitivity for DNA detection. Over the past years, considerable efforts have been paid on the development of chemical modified electrodes

* Corresponding author. Tel.: +86 376 6391825; fax: +86 376 6391825.
E-mail address: yfanchem@gmail.com (Y. Fan).

0013-4686/$ – see front matter © 2011 Elsevier Ltd. All rights reserved.
doi:10.1016/j.electacta.2011.02.114

to improve the electrochemical sensing performance for guanine and adenine [31–39]. Most recently, Dong and coworkers revealed that the free base of DNA have enhanced electrochemical reactivity at the graphene modified glassy carbon electrode [10]. Also, Pumera and coworker demonstrated that the stacked graphene nanofibers (SGNFs) have superior electrocatalytic activity for DNA oxidation over carbon nanotubes (CNTs) [40]. These results indicate that the graphene-based electrode materials are promising for electrochemical sensing of DNA.

Herein, we report the TiO_2-graphene nanocomposite prepared *via* hydrolysis of titanium isopropoxide in colloidal suspension of graphene oxide and in situ hydrothermal treatment. The as-prepared TiO_2-graphene nanocomposite exhibits remarkable electrocatalytic activity towards adenine and guanine oxidation. These two species can be simultaneously detected on the TiO_2-graphene modified GCE with high sensitivity in a wide linear range. This work offered a facile and efficient method to prepare TiO_2-graphene nanocomposite for electrochemical sensors application.

2. Experimental

2.1. Reagents and apparatus

Graphite powder (320 mesh, spectrographic pure) was purchased from Sinopharm Chemical Reagent Co., Ltd. Titanium isopropoxide ($Ti(O^iPr)_4$, 98%) was obtained from Aladdin Chemistry Co., Ltd. Adenine and guanine were purchased from Alfa Aesar. Herring sperm DNA (dsDNA) was obtained from Sigma Aldrich. All other chemicals were of analytical reagent grade and used as received. Water used throughout all experiments was purified with the Millipore system.

FT-IR spectra (KBr pellets) were recorded using a Bruker TENSOR27 instrument. Powder X-ray diffraction (XRD) data were collected on a Rigaku MiniFlex II X-ray diffractometer. Scanning electron microscopy (SEM) images were obtained on a Hitachi S-4800 scanning electron microscope. All electrochemical experiments were performed with a CHI 660C electrochemical workstation (CH Instruments, Shanghai, China). A conventional three-electrode system was used for all electrochemical experiments, which consisted of a platinum wire as counter electrode, an Ag/AgCl/3 M KCl as reference electrode, and a bare or modified glassy carbon electrode (3 mm diameter) as working electrode.

2.2. Preparation of TiO_2-graphene nanocomposite

Graphene oxide was prepared from graphite powder by the modified Hummers method [41,42]. In a typical preparation of TiO_2-graphene, 20 mg of graphene oxide was dispersed in a mixed solution of H_2O (10 mL) and ethanol (5 mL) under ultrasonication for 1 h to get a homogenous suspension of exfoliated graphene oxide. Then, 0.2 mL of $Ti(O^iPr)_4$ was added to the graphene oxide suspension and ultrasonicated for another 1 h. The resultant mixture was transferred to a 25 mL Teflon-sealed autoclave and kept in oven at 130 °C for 12 h. The final product was isolated by filtration, rinsed thoroughly with deionized water and ethanol, and dried in vacuum. The TiO_2-graphene nanocomposite was obtained in the form of black powder.

2.3. Preparation of modified electrode

The as-prepared TiO_2-graphene nanocomposite (2 mg) was dispersed in DMF (2 mL) with ultrasonic treatment for 1 h to get a homogenous dispersion (1 mg/mL). Then, 6 μL of the suspension was dropped onto the surface of freshly polished glassy carbon electrode and dried at room temperature to get the TiO_2-graphene modified GCE (TiO_2-graphene/GCE). For comparison, 6 μL of the homogenous suspension of graphene in DMF (1 mg/mL) was also coated on bare GCE to obtain the graphene modified GCE (graphene/GCE).

2.4. Preparation of DNA samples

Thermally denatured dsDNA was prepared according to the literature method [36]. Briefly, the native herring sperm dsDNA solution was heated in a boiling water bath at 100 °C for about 10 min, and then it was rapidly cooled in an ice bath. This kind of thermally denatured dsDNA can be used as single-stranded DNA (ssDNA).

2.5. Voltammetric procedure

The electrochemical measurements were performed in 0.1 M HAc-NaAc (pH 4.5) buffer solution with different concentrations of adenine and guanine. The solution pH was optimized in the range of 4.06–6.05 (Fig. S1) with the maximum voltammetric response occurred at pH 4.45. The accumulation potential was then optimized from −0.6 to 0.4 V with the maximum voltammetric response obtained at −0.4 V (Fig. S2). Thus, the accumulation of adenine and guanine at the working electrode was done in a stirred solution at −0.4 V. The effect of accumulation time was also investigated. The peak currents of adenine and guanine increased with the accumulation time within 100 s, and remained almost constant after 100 s, indicating the surface adsorption saturation. For practical purposes, a 100 s accumulation period was sufficient for the determination.

3. Results and discussion

3.1. Preparation and characterization of TiO_2-graphene nanocomposite

In this work, graphene oxide was firstly exfoliated in a mixed solution of water and ethanol under ultrasonication to produce colloidal suspension of graphene oxide. Intercalation and graft of titanium isopropoxide was then carried out in the graphene oxide suspension by ultrasonic treatment. Afterwards, TiO_2-graphene nanocomposite was obtained through hydrothermal treatment to reduce graphene oxide with in situ crystallization and immobilization of TiO_2 nanoparticles on graphene substrates. FT-IR spectra of the as-prepared TiO_2-graphene nanocomposite exhibit an intense low frequency absorption band around 610 cm^{-1} (Fig. S3), which clearly represents the vibration of Ti–O bonds in TiO_2 [25]. The absorption band appearing at 1590 cm^{-1} shows the skeletal vibration of graphene sheets [43], indicating the reduction of graphene oxide to graphene during the hydrothermal process. The XRD patterns of the as-prepared TiO_2-graphene are given in Fig. 1. The peaks in this diffraction patterns correspond to the anatase phase of TiO_2 (JCPDS file no. 21-1272), suggesting the complete formation of anatase TiO_2 during the hydrothermal process. However, the diffraction peaks of graphene are not distinguishable in XRD patterns of TiO_2-graphene. This phenomena has also been observed in other relevant works, and it can be ascribed to the much lower crystalline extent of graphene than that of TiO_2, which results in the shielding of the graphene peaks by those of TiO_2 [25]. Fig. 2 shows the SEM image of the as-prepared TiO_2-graphene nanocomposite. The integration between TiO_2 and graphene can be visualized from the SEM image, in which TiO_2 nanoparticles at the size of *ca.* 20–30 nm are uniformly and compactly embedded on the graphene substrate. It has been demonstrated that graphene oxide is heavily oxygenated, bearing hydroxyl and epoxide groups on its basal planes and carboxyl groups at the sheet edges [44]. These oxygen containing groups can effectively interact with the hard Ti^{4+} Lewis

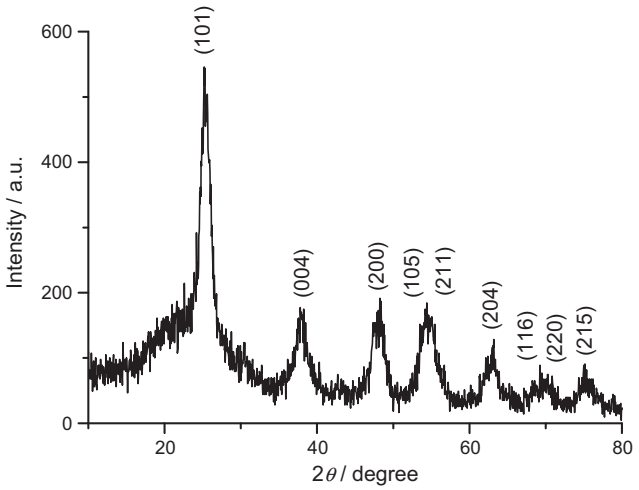

Fig. 1. XRD patterns of TiO_2-graphene nanocomposite.

acid, which promotes the intercalation of Ti species into graphene oxide layers [27,28]. Afterwards, under the hydrothermal process, graphene oxide can be reduced to graphene with in situ immobilization of TiO_2 nanoparticles on the resultant graphene sheets.

3.2. Electrochemical behavior of adenine and guanine

Fig. S4 depicts the cyclic voltammograms (CVs) of adenine (20 μM) and guanine (20 μM) on the TiO_2-graphene/GCE in 0.1 M HAc-NaAc (pH 4.5). It can be seen that G and A exhibit well-defined oxidation peak at 0.97 V and 1.26 V, respectively. No reduction peaks can be observed on the cathodic scan, which indicates the electrochemical oxidation of G and A on the TiO_2-graphene composite film is an irreversible process. The differential pulse voltammograms (DPVs) of the binary mixture of G and A on the bare GCE, graphene/GCE and TiO_2-graphene/GCE are given in Fig. 3. The DPV peak potential of G at the bare GCE and graphene/GCE is located at 0.99 and 0.92 V, respectively. In the case of TiO_2-graphene/GCE, the peak potential is negatively shifted to 0.88 V, and the peak current significantly increases to 2.4 μA. For adenine, the oxidation peak potential on TiO_2-graphene/GCE is also negatively shifted to 1.19 V, and the peak current increases up to 3.18 μA. Thus, the enhancement on the peak current and lowering of oxidation overpotential are clear evidence of the electrocatalytic activity of TiO_2-graphene towards the oxidation of guanine and adenine.

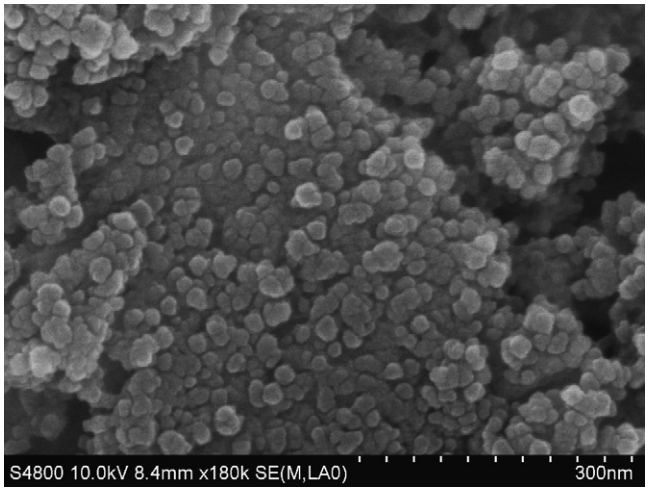

Fig. 2. SEM image of TiO_2-graphene nanocomposite.

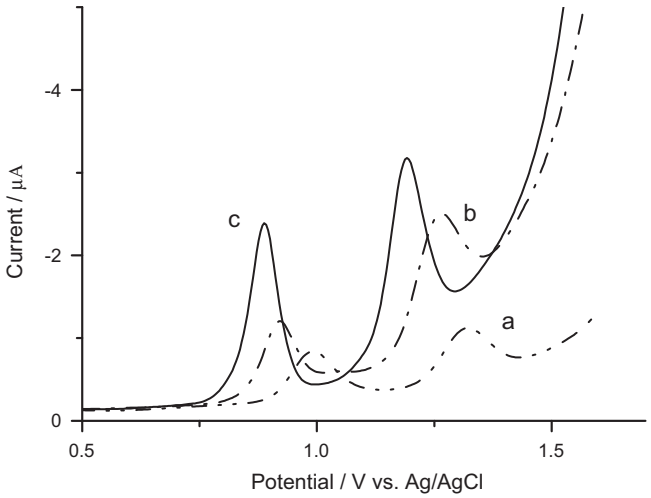

Fig. 3. DPVs of the mixture containing 20 μM adenine and 20 μM guanine on (a) the bare GCE, (b) graphene/GCE and (c) TiO_2-graphene/GCE in 0.1 M HAc-NaAc (pH 4.5).

Cyclic voltammograms of guanine and adenine at various scan rates on the TiO_2-graphene/GCE was also investigated. As shown in Fig. 4, at scan rates in the range of 50–600 mV s^{-1}, the oxidation peak currents increase linearly with scan rates, suggesting that

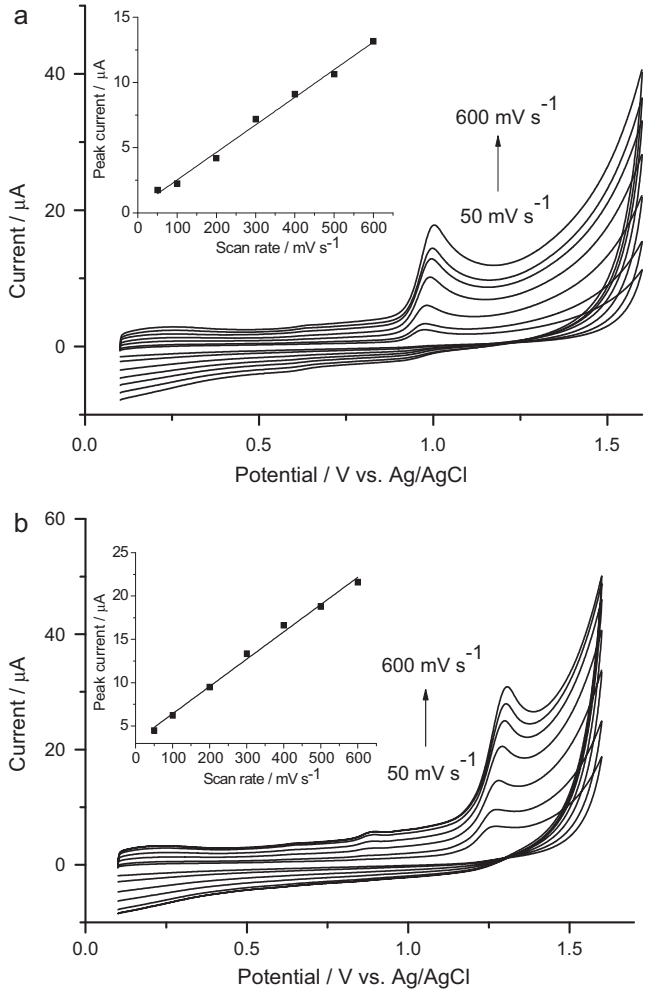

Fig. 4. CVs of (a) 20 μM guanine and (b) 20 μM adenine on the TiO_2-graphene/GCE in 0.1 M HAc-NaAc (pH 4.5) at different scan rates from 50 to 600 mV s^{-1}. Insert, the plot of the oxidation peak current vs. scan rate.

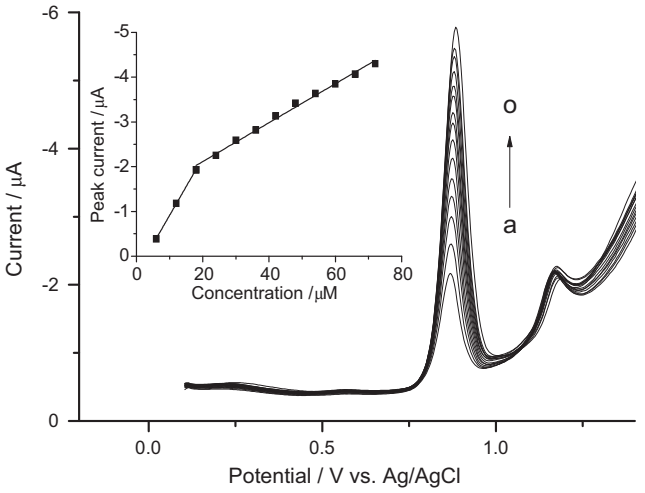

Fig. 5. DPVs of 8, 12, 16, 20, 26, 28, 36, 40, 44, 48, 52, 56, 60, 64 and 68 μM guanine (from a to o) in the presence of 8 μM adenine on TiO_2-graphene/GCE in 0.1 M HAc-NaAc (pH 4.5). Insert, the plot of the peak current vs. guanine concentration.

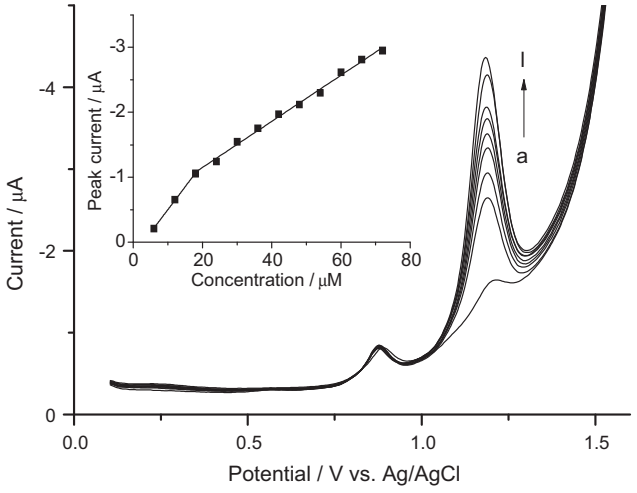

Fig. 6. DPVs of 6, 12, 18, 24, 30, 36, 42, 48, 54, 60, 66 and 72 μM adenine (from a to l) on TiO_2-graphene/GCE in the presence of 6 μM guanine in 0.1 M HAc-NaAc (pH 4.5). Insert, the plot of the peak current vs. adenine concentration.

the electrochemical oxidation of G and A at TiO_2-graphene/GCE is a surface-controlled process. The linear regression equation is expressed as: $I_{pa}/\mu A = 0.4052 + 0.02115\,\nu/mV\,s^{-1}$ ($R = 0.9961$) and $I_{pa}/\mu A = 3.279 + 0.03147\,\nu/mV\,s^{-1}$ ($R = 0.9964$) for G and A, respectively. Furthermore, the electron transfer rate constant (k_s) at the TiO_2-graphene composite film can be estimated using the Laviron's model [45]. As shown in Fig. S5, plotting the E_{pa} vs. $\log\nu$ produces a straight line with the slop of $2.3RT/(1-\alpha)nF$ at high scan rates, and the linear regression equation is expressed as: $E_{pa}/V = 1.012 + 0.04177\log\nu/V\,s^{-1}$ ($R = 0.9916$) and $E_p/V = 1.319 + 0.05485\log\nu/V\,s^{-1}$ ($R = 0.9973$) for G and A, respectively. From the value of the slop, the electron transfer coefficient (α) is estimated to be 0.45 (G) and 0.29 (A). According to the Laviron equation: $\log k_s = \alpha\log(1-\alpha) + (1-\alpha)\log\alpha - \log(RT/nFv) - \alpha(1-\alpha) - \log(nF\Delta E_p/2.3RT)$, the k_s is calculated to be 2.51 and 2.13 s^{-1} for G and A, respectively. This k_s is comparable with that on Mo(VI) complex–TiO_2 nanoparticle modified carbon paste electrode (3.83 s^{-1}) [33], and it is much higher than that previously reported on carbon ionic liquid electrode (7.42×10^{-4} s^{-1} for A and 2.39×10^{-3} s^{-1} for G) [36]. These results demonstrate that the TiO_2-graphene nanocomposite significantly facilitates the electron transfer kinetics and promotes the electrochemical oxidation of these small biomolecules.

The electrochemical oxidation of guanine and adenine involves a two-proton and two-electron process in the rate determining step [38]. In this study, it is observed that the oxidation peak potential of G and A shift negatively with the increment of solution pH in the range of 4.00–6.05, and the pH dependence of E_p can be expressed by the linear regression equations as: $E_p/V = 1.148 - 0.05613pH$ ($R = 0.9905$) and $E_p/V = 1.518 - 0.06611pH$ ($R = 0.9956$) for G and A, respectively (Fig. S6). The calculated slope of 0.05613 V/pH (A) and 0.06611 V/pH (G) are close to the theoretical value of 0.0586 V/pH according to the Nernst equation [46], suggesting that the direct electrooxidation of G and A on the TiO_2-graphene/GCE is a two-proton and two-electron process.

3.3. Determination of adenine and guanine

The electrochemical sensing performance of the TiO_2-graphene/GCE towards guanine and adenine detection was investigated by DPV in the optimized conditions. Selective determination of G and A was carried out in their binary mixture with one species maintaining at a constant concentration. Fig. 5 shows the DPVs of various concentration of G in the presence of a fixed concentration of A (8 μM). It can be seen that the peak current of G increases with the increasing concentration, while the peak current of A almost holds constant. The calibration curve for G shows two linear segments: the first linear segment increases from 8 to 20 μM with the regression equation of $I_p/\mu A = 0.3748 - 0.1286c_G/\mu M$ ($R = 0.9997$), and the second linear segment increases up to 68 μM with the linear regression equation of $I_p/\mu A = -1.245 - 0.04344c_G/\mu M$ ($R = 0.9967$). The same appears to be the case when A coexists with G (6 μM) in the range of 6–72 μM, with the regression equation of $I_p/\mu A = -2.054 - 0.07062c_A/\mu M$ ($R = 0.9992$) and $I_p/\mu A = -0.4399 - 0.03551c_A/\mu M$ ($R = 0.9975$) at the turn of 18 μM (Fig. 6). It has also been observed in earlier reports that the calibration curve of A and G detection usually divided into two linear regions [34,37]. The first linear region in the calibration curve can be ascribed to an absorption process of A or G on the modified electrode surface, and the second linear region may be attributed a diffusion process on the monolayer-covered surface [37].

Since adenine and guanine are the coexisting purine bases in DNA, simultaneous determination of these two species is an important performance for DNA detection from the practical application point of view. Simultaneous determination of various concentrations of G and A was carried out on the TiO_2-graphene/GCE under the optimized conditions. As shown in Fig. 7, the calibration curves for G and A also exhibit two linear segments with regression equation as: $I_p/\mu A = -0.2933 - 0.1150c_G/\mu M$ ($R = 0.9918$) (0.5–20 μM) and $I_p/\mu A = -1.992 - 0.03325c_G/\mu M$ ($R = 0.9992$) (20–200 μM) for G; and $I_p/\mu A = -0.3586 - 0.1078c_A/\mu M$ ($R = 0.9950$) (0.5–20 μM) and $I_p/\mu A = -1.963 - 0.03121c_A/\mu M$ ($R = 0.9981$) (20–200 μM) for A. These results indicate that, on the TiO_2-graphene composite film, the competitive adsorption equilibrium can be attained at the suitable concentrations of guanine and adenine. Therefore, the guanine and adenine could be determined simultaneously from a mixture in large concentration domains by the proposed method. The linear detection range for both A and G is 0.5–200 μM, which is much wider than the previously reported electrochemical sensors [34–39]. The detection limit (S/N = 3) for A and G was calculated to be 0.10 μM and 0.15 μM, respectively. This excellent electrochemical sensing performance can be ascribed to the good adsorptivity, antifouling property and high electron transfer kinetics of the TiO_2-graphene nanocomposite, which provide an

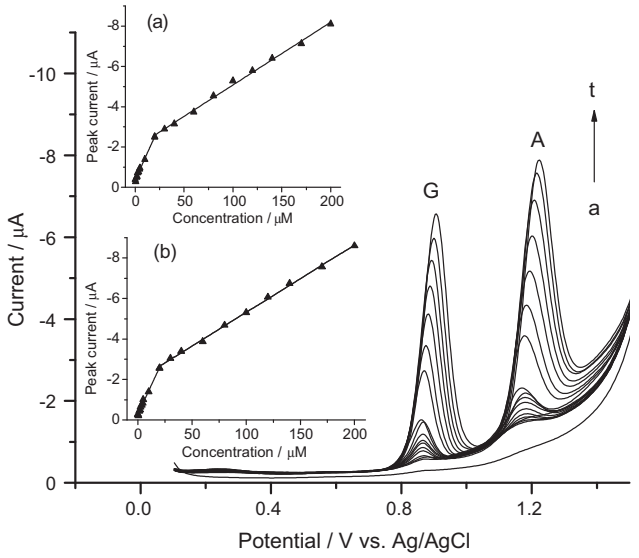

Fig. 7. DPVs of 0, 0.5, 1.0, 1.5, 2.0, 2.5, 3.5, 4.5, 5.5, 10, 20, 30, 40, 60, 80, 100, 120, 140, 170 and 200 μM adenine and guanine (from a to t) in 0.1 M HAc-NaAc (pH 4.5). Insert, (a) the plot of the peak current vs. adenine concentration, and (b) the plot of the peak current vs. guanine concentration.

efficient microenvironment for electrochemical reaction of these purine bases.

3.4. Stability and reproducibility of the modified electrode

The long-term stability of the TiO_2-graphene/GCE electrochemical sensor was investigated by examining its current response during storage in a refrigerator at 4 °C. The electrochemical sensor exhibited no obvious decrease in current response in the first week and maintained about 92% of its initial value after two weeks. The relative standard deviation (RSD) of the TiO_2-graphene/GCE in response to 1.0 μM adenine and 1.0 μM guanine for ten measurements was 4.6% and 4.1%, respectively, indicating the good reproducibility. The possible interference for voltammetric determination of guanine and adenine at the TiO_2-graphene/GCE was investigated. No substantial change in voltammetric response of both the analyte (20 μM) was observed in the presence of 10-fold concentration of ascorbic acid, uric acid and dopamine.

3.5. Analytical applications

The TiO_2-graphene/GCE electrochemical sensor was applied to detect the adenine and guanine content of thermally denatured DNA. In a typical procedure, 20 μL of the thermally denatured DNA was added to a cell containing 5 mL buffer solution, and then the peak currents of adenine and guanine residues were measured. Afterwards, 20 μM adenine and 20 μM guanine was added to the above solution and the peak currents were recorded again. Using the calibration curves obtained previously in simultaneous determination of adenine and guanine, the concentrations of A and G in DNA can be calculated from peak currents. The contents of A and G in the thermally denatured DNA were calculated to be 22.0 mol% and 27.4 mol%, respectively. The value of (G + C)/(A + T) was obtained as 0.80, which was close to the standard value of 0.77 [47].

4. Conclusions

In conclusion, we have demonstrated a facile and effective method for the preparation of TiO_2-graphene nanocomposite. This synthetic approach consists of intercalation and graft of titanium isopropoxide on graphene oxide sheets, and the hydrothermal treatment to immobilize TiO_2 nanoparticles on the graphene substrate. The as-prepared TiO_2-graphene nanocomposite modified glassy carbon electrode exhibits remarkable electrocatalytic activity towards adenine and guanine oxidation. The good adsorptivity and conductivity of TiO_2 greatly improved the electrochemical sensing performance. Using the fabricated TiO_2-graphene/GCE electrochemical sensor, adenine and guanine can be detected simultaneously with low detection limit and wide linear range. This work indicates that the TiO_2-graphene nanocomposite has great potential for applications in constructing cost-effective and high performance electrochemical sensors.

Acknowledgements

This work was financially supported by the National Natural Science Foundation of China (No. 21002082), the Key Project of Chinese Ministry of Education (No. 210129), the Program for Science & Technology Innovation Talents in Universities of He'nan Province (No. 2010HASTIT025), the key Technology R&D Program of He'nan Province (No.082100234005), and the Excellent Youth Foundation of He'nan Scientific Committee (No. 104100510020).

Appendix A. Supplementary data

Supplementary data associated with this article can be found, in the online version, at doi:10.1016/j.electacta.2011.02.114.

References

[1] Y. Shao, J. Wang, H. Wu, J. Liu, I.A. Aksay, Y. Lin, Electroanalysis 22 (2010) 1027.
[2] M. Pumera, A. Ambrosi, A. Bonanni, E.L.K. Chng, H.L. Poh, Trends Anal. Chem. 29 (2010) 954.
[3] D. Chen, L. Tang, J. Li, Chem. Soc. Rev. 39 (2010) 3157.
[4] M. Pumera, Chem. Soc. Rev. 39 (2010) 4146.
[5] J. Lu, L.T. Drzal, R.M. Worden, I. Lee, Chem. Mater. 19 (2007) 6240.
[6] C. Shan, H. Yang, J. Song, D. Han, A. Ivaska, L. Niu, Anal. Chem. 81 (2009) 2378.
[7] X. Kang, J. Wang, H. Wu, I.A. Aksay, J. Liu, Y. Lin, Biosens. Bioelectron. 25 (2009) 901.
[8] J.F. Wu, M.Q. Xu, G.C. Zhao, Electrochem. Commun. 12 (2010) 175.
[9] K. Liu, J. Zhang, G. Yang, C. Wang, J.J. Zhu, Electrochem. Commun. 12 (2010) 402.
[10] M. Zhou, Y. Zhai, S. Dong, Anal. Chem. 81 (2009) 5063.
[11] N.G. Shang, P. Papakonstantinou, M. McMullan, M. Chu, A. Stamboulis, A. Potenza, S.S. Dhesi, H. Marchetto, Adv. Funct. Mater. 18 (2008) 3506.
[12] Y. Wang, Y. Li, L. Tang, J. Lu, J. Li, Electrochem. Commun. 11 (2009) 889.
[13] S. Alwarappan, A. Erdem, C. Liu, C.Z. Li, J. Phys. Chem. C 113 (2009) 8853.
[14] P.V. Kamat, J. Phys. Chem. Lett. 1 (2010) 520.
[15] S. Guo, D. Wen, Y. Zhai, S. Dong, E. Wang, ACS Nano 4 (2010) 3959.
[16] C. Shan, H. Yang, D. Han, Q. Zhang, A. Ivaska, L. Niu, Biosens. Bioelectron. 25 (2010) 1070.
[17] P. Benvenuto, A.K.M. Kafi, A. Chen, J. Electroanal. Chem. 627 (2009) 76.
[18] Y. Zhu, H. Cao, L. Tang, X. Yang, C. Li, Electrochim. Acta 54 (2009) 2823.
[19] Y. Luo, H. Liu, Q. Rui, Y. Tian, Anal. Chem. 81 (2009) 3035.
[20] L.C. Jiang, W.D. Zhang, Electroanalysis 21 (2009) 988.
[21] Y. Luo, Y. Tian, A. Zhu, Q. Rui, H. Liu, Electrochem. Commun. 11 (2009) 174.
[22] H. Tang, F. Yan, Q. Tai, H.L.W. Chan, Biosens. Bioelectron. 25 (2010) 1646.
[23] A. Liu, M. Wei, I. Honma, H. Zhou, Adv. Funct. Mater. 16 (2006) 371.
[24] S.J. Bao, C.M. Li, J.F. Zang, X.Q. Cui, Y. Qiao, J. Guo, Adv. Funct. Mater. 18 (2008) 591.
[25] H. Zhang, X. Lv, Y. Li, Y. Wang, J. Li, ACS Nano 4 (2010) 380.
[26] D. Wang, D. Choi, J. Li, Z. Yang, Z. Nie, R. Kou, D. Hu, C. Wang, L.V. Saraf, J. Zhang, I.A. Aksay, J. Liu, ACS Nano 4 (2010) 907.
[27] Y.B. Tang, C.S. Lee, J. Xu, Z.T. Liu, Z.H. Chen, Z. He, Y.L. Cao, G. Yuan, H. Song, L. Chen, L. Luo, H.M. Cheng, W.J. Zhang, I. Bello, S.T. Lee, ACS Nano 4 (2010) 3482.
[28] T.N. Lambert, C.A. Chavez, B. Hernandez-Sanchez, P. Lu, N.S. Bell, A. Ambrosini, T. Friedman, T.J. Boyle, D.R. Wheeler, D.L. Huber, J. Phys. Chem. C 113 (2009) 19812.
[29] Y. Fan, H.T. Lu, J.H. Liu, C.P. Yang, Q.S. Jing, Y.X. Zhang, X.K. Yang, K.J. Huang, Colloids Surf. B 83 (2011) 78.
[30] J. Wang, Anal. Chim. Acta 469 (2002) 63.
[31] C. Tang, U. Yogeswaran, S.M. Chen, Anal. Chim. Acta 636 (2009) 19.
[32] F. Xiao, F. Zhao, J. Li, L. Liu, B. Zeng, Electrochim. Acta 53 (2008) 7781.
[33] M.M. Ardakani, Z. Taleat, H. Beitollahi, M. Salavati-Niasari, B.B.F. Mirjalili, N. Taghavinia, J. Electroanal. Chem. 624 (2008) 73.
[34] H.S. Wang, H.X. Ju, H.Y. Chen, Anal. Chim. Acta 461 (2002) 243.
[35] A. Abbaspour, A. Ghaffarinejad, Electrochim. Acta 55 (2010) 1090.
[36] W. Sun, Y. Li, Y. Duan, K. Jiao, Biosens. Bioelectron. 24 (2008) 988.

[37] J.M. Zen, M.R. Chang, G. Ilangovan, Analyst 124 (1999) 679.
[38] Z. Wang, S. Xiao, Y. Chen, J. Electroanal. Chem. 589 (2006) 237.
[39] K.J. Huang, D.J. Niu, J.Y. Sun, C.H. Han, Z.W. Wu, Y.L. Li, X.Q. Xiong, Colloids Surf. B 82 (2011) 543.
[40] A. Ambrosia, M. Pumera, Phys. Chem. Chem. Phys. 12 (2010) 8943.
[41] W.S. Hummers, R.E. Offeman, J. Am. Chem. Soc. 80 (1958) 1339.
[42] N.I. Kovtyukhova, P.J. Ollivier, B.R. Martin, T.E. Mallouk, S.A. Chizhik, E.V. Buzaneva, A.D. Gorchinskiy, Chem. Mater. 11 (1999) 771.
[43] C. Nethravathi, M. Rajamathi, Carbon 46 (2008) 1994.
[44] S. Park, R.S. Ruoff, Nat. Nanotechnol. 4 (2009) 217.
[45] E. Laviron, J. Electroanal. Chem. 101 (1979) 19.
[46] A.J. Bard, L.R. Faulkner, Electrochemical Methods: Fundamentals and Applications, 2nd ed., Wiley, New York, 2001.
[47] N. Davidson, The Biochemistry of the Nucleic Acids, 7th ed., Cox & Nyman, UK, 1972.